Detection of honey bees (*Apis mellifera*) in hypertemporal LiDAR point cloud time series to extract bee activity zones and times

Jannik S. Meyer[1], Ronald Tabernig[1,2], Bernhard Höfle[1,2]

[1] 3DGeo Research Group, Institute of Geography, Heidelberg University – jannik.meyer@stud.uni-heidelberg, (ronald.tabernig, hoefle)@uni-heidelberg.de
[2] Interdisciplinary Center for Scientific Computing (IWR), Heidelberg University

Keywords: LiDAR, Terrestrial Laser Scanning, Random Forest Classifier, Honey Bee Detection, Time Series.

Abstract

Given the vital role bees play in our ecosystems and their increasing endangerment, it is highly important to develop new methods that assist in gaining a deeper understanding of the spatial dimension of insect behavior. Conventional methods for monitoring bees are subject to accuracy limitations, experimental setup complexity, and lack the explicit spatial dimension. This study presents a novel approach for detecting and identifying honey bees (*Apis mellifera*) and Asian hornets (*Vespa velutina*) using hypertemporal LiDAR point clouds. We employed an experimental setup of a permanent terrestrial laser scanner (Riegl VZ-600i) to capture point clouds in a region of interest of 3 x 2 x 5 m at regular intervals (30 s) over ca. 1.8 h. By training a random forest classifier based on local neighbourhood features, the classified points can then be clustered in single and distinct objects of bees/hornets. Ultimately, a simple logical operator is employed to ascertain whether an object is a bee or hornet, according to definable knowledge-driven thresholds (e.g., size of bees). Our proposed method demonstrates high accuracy and precision in bee (n = 7,084, acc. = 97.44%, prec. = 99.07%) and hornet detection (n = 296, acc. = 87.71%, prec. = 67.65%), offering a fully automatic and 3D spatial monitoring alternative to traditional techniques. Furthermore, it allows for the identification of insect activity zones and times, as well as their relative change over time. We could identify zones of bee activity in front of the hive with observable flying slowdowns before entering and defensive behaviors in response to predators. This approach provides new insights into the spatial and temporal dynamics of insect populations, especially in the context of environmental and climate change.

1. Introduction

Bees are an essential species for maintaining the health of ecosystems, performing a range of ecological functions, particularly as pollinators of plants (Brown and Paxton, 2009). In many parts of the world European honey bees (*Apis mellifera*) are regarded as a key species, playing a significant role in agriculture. This includes the production of honey and the pollination of crops. In other words: bees fulfill a crucial role in food security and ecosystem conservation (Hung et al., 2018). However, honey bees and other wild bee species are particularly vulnerable to the impacts of climate change and anthropogenic alterations to landscapes and ecosystems (Vercelli et al., 2021, Tennakoon, 2024 and Rodet and Henry, 2014). Severe effects (e.g., declining populations, higher risk of diseases, etc.) are already observed by beekeepers and farmers around the world (Vercelli et al., 2021 and Brown and Paxton, 2009).

An understanding of the flying behavior of honey bees is crucial for comprehending their spatio-temporal distribution and interactions with the environment. Honey bees are known for their complex foraging patterns, which are influenced by a variety of environmental factors, including temperature, floral availability, and the presence of other pollinators (Ropars et al., 2019). These factors directly impact the flight behavior of the bees, which, in turn, affects their pollination efficiency and survival rates.

To gain a deeper insight into the underlying causes of behavioral change, it is essential to examine the bees in relation to a range of parameters, including the number of bees per colony, flight distances, flight duration, swarming period and so forth. A study conducted by Rodet and Henry (2014) investigated the flight distances of honey bees in changing landscapes. However, a significant challenge in such studies is the experimental setup and the associated effort, given that bees are relatively small and have a high level of mobility. This often necessitates the use of individual bees as the unit of observation, employing techniques such as RFID tracking (He et al., 2016) or manual counting (Rodet and Henry, 2014) to measure the entry and exit times of the hive.

The objective of this paper is to address these methodological constraints with often invasive setups, and propose a novel approach for measuring the number of bees and their spatio-temporal distribution using LiDAR technology. We employ a static terrestrial laser scanner (TLS) to scan a predefined area at regular intervals. The generated data is analyzed with an algorithm that integrates machine learning techniques. This allows for the identification of individual bees and hornets in the scene and the utilization of the number of bees and hornets as well as their spatial information to determine indices of activity. In other words, our method uses a time series of TLS point clouds as input and the outputs are detected individual bees and hornets as single objects in space and time, their spatial and temporal activity zones in 3D and their relative change over time. Our study serves as a scientific proof-of-concept of potential future application of permanent TLS (PLS) to monitor bees in particular, and insects in general. This could assist biologists in gaining a deeper understanding of the flight patterns and spatial as well as temporal distribution of bees, which could potentially be extended to even more insects. Furthermore, it could benefit beekeepers in enhancing their understanding of colony behavior and the early detection of attacks by predators (e.g., hornets) or the impact of other disruptive factors (e.g., climatic stress, pollution, weather, etc.).

2. State of the Art

The monitoring of individual bees can be accomplished by manually observing an area and consequently counting the bees or by outfitting the insects with miniature radio frequency identification (RFID) tags and measuring the times of entry and exit (Rodet and Henry, 2014 and He et al., 2016). For example, He et al. (2016) used this experimental setup to ascertain how the weather of the subsequent day exerts an influence on the foraging activities of the current day. By employing an individual animal tracking approach, they were able to demonstrate the impact of impending weather conditions on foraging duration and times. Shimasaki et al. (2020) used a video-based approach, utilizing high-frame-rate videos (500 fps) and detecting brightness fluctuations in pixels surrounding the wings to identify them. A similar video-based approach was used by Sun and Gaydecki (2021), which used image processing tools to track individual bees. Another approach to determine the location of insects and to distinguish between different species is used by Rydhmer et al. (2022) who are using a Scheimpflug LiDAR to measure a transect along a white clover field. In the general context of animal counting, Azmy et al. (2012) employed time-of-flight LiDAR technology to scan a cave where two colonies of distinct bat species were residing. By utilizing an automatic detection algorithm that considers the varying reflectance values between the bats' fur and the cave's surface as a detection criterion, they were able to map the bats within the cave and distinguish between the different species. This example also outlines the strengths of using an active monitoring system with LiDAR that is also working in weak/no-light conditions, which is not possible with video-based approaches. Given the feasibility of employing LiDAR technology to detect animals in general and the shown potential for insect observation in the literature, this study investigates the research gap on the utilization of a standard surveying LiDAR device for bee and hornet detection in space and time. This will be the first proof-of-concept study on PLS to derive near real-time spatio-temporal information for beekeepers and scientists.

3. Methods and Data

Our method to detect bees in hypertemporal LiDAR scenes is primarily motivated by the objective to develop a method that exclusively relies on spatial characteristics and relationships to accurately identify individual points in the point cloud and group them as distinct bees. Our workflow can be described by a four-step procedure: 1) the acquisition of data; 2) the pre-processing of the data; 3) the training of a machine learning model; 4) the application of a detection algorithm and the error assessment of the results. To address the challenge, a machine learning model is trained on a range of spatial features related to the local structure of the point cloud neighborhood, coupled with a clustering algorithm, to categorize individual points as bees or hornets. Subsequently, these points can be grouped and abstracted as distinct insects, paving the way for further analysis.

3.1 Measurement Setup and Data

The 4D (3D + time) point cloud dataset was acquired in the zoo of Heidelberg on September 16, 2024, between 2:54 p.m. and 4:47 p.m. as a near-continuous TLS time series. The scanning was conducted using a Riegl VZ-600i, with a nominal point spacing of 0.4 mm at a distance of 3 m, a pulse repetition rate of 2,200 kHz and a horizontal field of view of 40°. This resulted in a median point spacing of 1.1 mm in the ROI and a scan duration of 15 seconds. The scanning was conducted every 30 s, resulting in 225 epochs. As illustrated in Fig. 1, the scanner was situated at an approximate distance of 3 m from the beehive throughout the scanning process. Moreover, the scanner was aligned with the front of the hive and scanned the front of the hive. This yielded an area of ca. 6 m^2 in front of the hive.

Figure 1. Experimental setup in the zoo of Heidelberg (Date: 16 September 2024, photo: J. Meyer).

With this TLS setup we were able to capture flying bees in the acquired data. The bees appear as a spatial cluster of points in the point clouds with a size between 10 mm and 30 mm and consist of 10-75 points. While the hornets are approx. 50 mm in size and consist of 150-850 points. Due to the high velocity of the insects and the movement of the scanner, they may be distorted in their point cloud representation (cf. Weiser and Höfle, 2024). Nevertheless, they remain discernible and identifiable as bees/hornets. Examples are provided in Fig. 2.

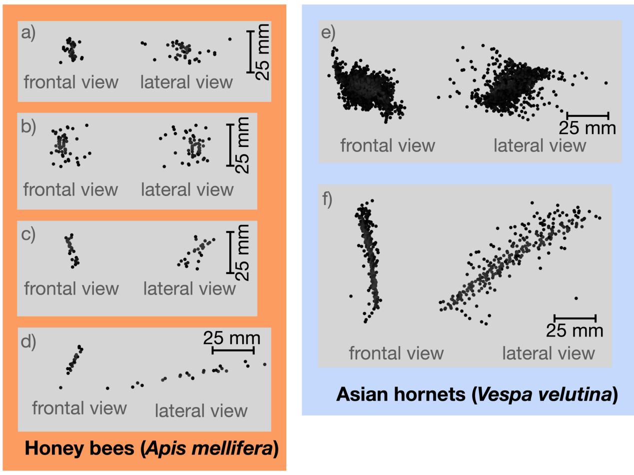

Figure 2. Example point clouds of honey bees (left) and Asian hornets (right) (front view is equal to the view of scanner and lateral view is orthogonal to that).

Additionally, the invasive species of Asian hornet (*Vespa velutina*), which is not native to Germany, was identified in front of the hive. Consequently, they were also discernible in the point clouds and matched the observations made during acquisition with regard to their location in space and time (Fig. 2 and 3).

3.2 Workflow

To accomplish the objective of detecting and identifying bees and hornets in LiDAR point cloud time series, an algorithm was developed which classifies points in the point cloud based on a machine-learning classifier that has been trained on real, manually labeled data. A random forest (RF) classifier was used because it can easily handle high dimensionality of the data and the complex, non-linear relationships between the features, as well as the relatively small and imbalanced training dataset (Alfio et al., 2024 and Breiman, 2001). Additionally, neighborhood operations such as spatial clustering were utilized to group together and identify individual insects. This entailed a dual-stage process: first, the training of the RF model, and second, the detection algorithm. The schematic workflow is illustrated in Fig. 4.

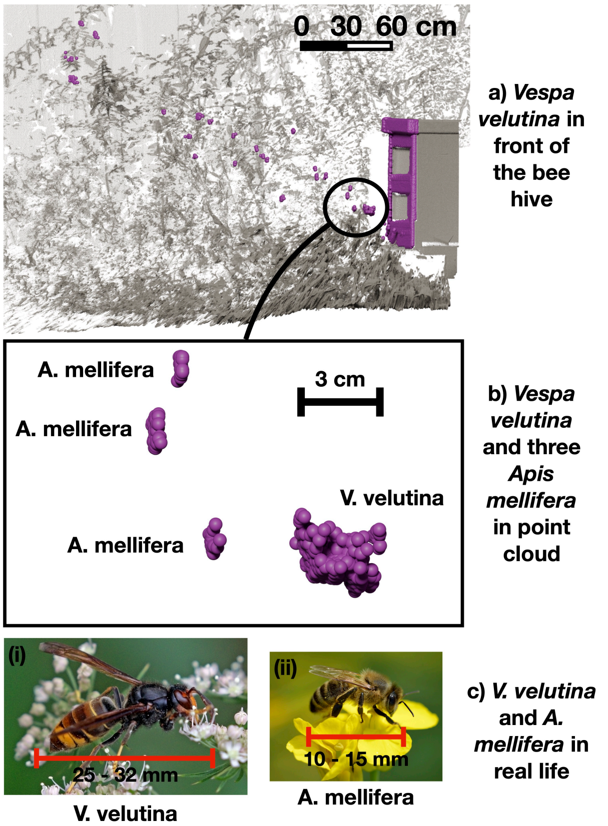

Figure 3. Asian hornet visible in point cloud (purple dots are LiDAR points within the ROI) of epoch 15:02:26 and image of Asian hornet (*V. velutina*) and honey bee (*A. mellifera*). Photos slightly modified from (i) Charles J. Sharp licensed under CC BY-SA 4.0, (ii) Ivar Leidus licensed under CC BY-SA 4.0).

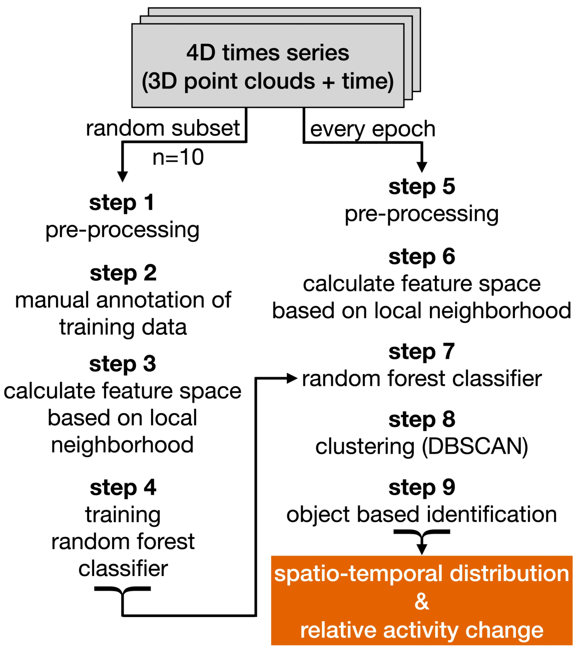

Figure 4. Workflow of the complete bee-detection algorithm.

3.2.1 Pre-processing

The data underwent a pre-processing step in the training and application phase (step 1, step 5 in Fig. 4), during which it was segmented to the area of interest. For this purpose, our open-source tool *VAPC* was employed (Tabernig et al., 2024). The tool was used to segment the individual scenes of the time series in accordance with a 3D mask. The 3D mask was defined by another point cloud, which was the point cloud scene without bees and hornets, and based on this scene the irrelevant "background" of the scene was removed: This "background" point cloud was first voxelized and then applied as a mask to each single scan. In comparison to a simple 3D bounding box approach, our technique allowed for the precise delineation of recurring objects, such as vegetation, while avoiding the removal of other points that would have been within the bounding box but not within the precise 3D mask (e.g., flying bees) (Fig. 5). This process was undertaken in order to only select the insects and thereby drastically reduced the amount of data for subsequent stages of the analysis.

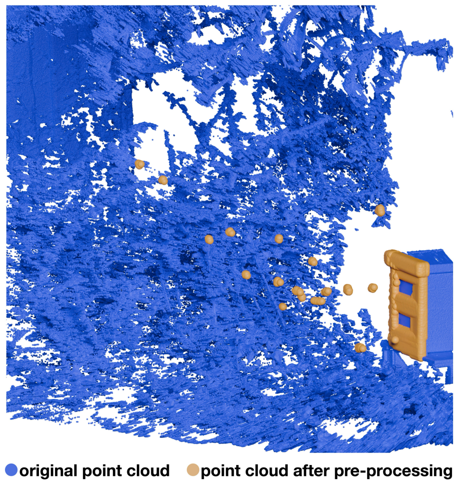

Figure 5. Pre-processing of example epoch (blue: mask point cloud, orange: points kept for further processing).

3.2.2 Random Forest Model

Our objective was to classify points in the LiDAR point clouds as either bees, hornets or miscellaneous (e.g., including ground, buildings, vegetation, etc.). To guarantee that the RF model was capable of differentiating between points belonging to bees, hornets and those that did not (i.e., miscellaneous), a manual training method was deemed the most appropriate. Prior to training the RF model, the point clouds underwent pre-processing (step 1). This entailed the selection based on 10 random scenes from the 4D point cloud dataset for training. These pre-processed scenes were then prepared for training through manual labelling (by visual comparisons of the photos captured by the scanner) of points (step 2) according to their respective classes (i.e., bees, hornets and miscellaneous). Over the 10 epochs there were 2,468,945 points classified as misc., 3,083 points as bees and 3,102 points classified as hornets, corresponding to 74 bees and 9 hornets in real life. Subsequently, the manually classified epochs were integrated into a dataset and incorporated into the training algorithm with target classes: 0 = bee, 1 = misc. and 2 = hornet.

In order to identify bees and hornets, it is necessary to describe the local properties of a given point in relation to the neighboring points, considering the geometric relationships that exist between them. Accordingly, the structure tensor, a 3x3 matrix obtained from the coordinates of the points near a query point, represents the structure of the local neighborhood. From this structure tensor, a total of seven different features were determined that showed characteristic values for the three different classes (step 3). The neighborhood query for every point in the point cloud (i.e., the neighborhood query) was performed by a fixed distance (r_s) search in 3D (Weinmann et al., 2013). Based on the set of neighboring points to any central point, the different features were conceptualized to represent class-distinctive characteristics (Mohamed et al., 2022). The equations for anisotropy, linearity, curvedness, omnivariance and eigenentropy were taken from Weinmann et al. (2013). With regard to the task of classifying points as bees/hornets/miscellaneous the three different classes could mainly be distinguished by types of features, which concerned the shape and characteristics of the local neighborhood. Therefore, following seven features were used which seemed suitable for the task of differentiating between bees, hornets and miscellaneous.

The initial feature is **anisotropy (A)**:

$$A = \frac{\lambda_1 - \lambda_3}{\lambda_1} \quad (1)$$

where λ_1 and λ_3 are the largest and smallest eigenvalues, respectively, derived from the covariance matrix of the neighboring points. For bees and hornets, this feature helped differentiate their flight in open air from denser, more complex objects like plants or hives, because of their small size compared to the query radius they showed low values for the anisotropy.

The second feature is **linearity (L)**:

$$L = \frac{\lambda_1 - \lambda_2}{\lambda_1} \quad (2)$$

where λ_2 is the second largest eigenvalue. For hornets and bees, which often exhibit more elongated shapes when in flight, this feature tends to be higher compared to more scattered or less structured point distributions, such as plants or hive surfaces.

The third feature, **curvedness (C)**:

$$C = \frac{\lambda_3}{\lambda_1 + \lambda_2 + \lambda_3} \quad (3)$$

This feature is particularly useful for detecting irregular or curved shapes, which some of the bees and hornets show.

The fourth feature is **omnivariance (O)**:

$$O = \sqrt[3]{\lambda_1 \cdot \lambda_2 \cdot \lambda_3} \quad (4)$$

High omnivariance indicates a three-dimensional, volumetric distribution of points, which is expected for the plants and hives. In contrast, bees and hornets in flight, due to their more defined and smaller shapes, typically exhibit lower omnivariance values.

The fifth feature is **eigenentropy (E)**:

$$E = -\sum_{i=1}^{3} \lambda_i \, \log(\lambda_i) \quad (5)$$

where λ_i are the eigenvalues of the covariance matrix. Eigenentropy provides insight into how uniformly the points are distributed around the central point. Higher entropy values indicate a more disordered or complex neighborhood, typical for highly variable structures like plants, while lower values are indicative of more ordered or regular point distributions, such as those point signatures produced by bees and hornets.

The sixth feature is **mean quadratic distances to the center of gravity (R_{cog})**, which measures the spatial spread of the points around the center of the local neighborhood. It is calculated as:

$$R_{cog} = \frac{1}{N}\sum_{i=1}^{N} \|x_i - \bar{x}\|^2 \quad (6)$$

where N is the number of neighboring points, x_i is the position of each point, and $\bar{x}$ is the center of mass of the neighborhood. So, this feature quantifies the size of the local neighborhood, capturing the absolute spatial extent of points around the central point. Which means larger values of R_g are associated with bigger local point distributions, while smaller values correspond to more concentrated or compact distributions around the center of gravity. This is especially useful to distinguish between bees and hornets due to their different typical sizes (Fig. 2).

The seventh feature is the **local density (ρ)** and represents how many points are located in a certain volume (which is based on the radius of the neighborhood definition) around the central point.

$$\rho = \frac{N}{\frac{3}{4}\pi r^2} \quad (7)$$

Based on the knowledge on the different sizes between bees and hornets as well as the fact that they are flying in the air, the density values of points classified as bees or hornets are quite low compared to miscellaneous points. This makes this feature helpful for the classification of the LiDAR data.

Once these features were computed, the RF classifier was employed to perform supervised learning based on the dataset of pre-classified epochs (step 4 in Fig. 4). The model was trained to recognize patterns in the feature space that correspond to the presence of bees and hornets, allowing it to classify new, unseen data effectively (step 7 in Fig 4).

Parameter settings: In order to accurately identify bees and hornets, it was essential to set the parameters of the RF classifier to realistic and semantically meaningful values. The most significant and important parameter is the radius for the neighbor query (r_s), which was set to 50 mm. This value is justified by the fact that the average size of a honey bee (*Apis mellifera*) is approximately 11-16 mm (Pertischak, 2021). This implies that, for a given point, the neighborhood operations were performed using at least the points that are part of the same bee, and at least every point within a sphere with a radius that is four-and-a-half-times larger than the length of an actual bee. This condition resulted from the different possible point signatures which can be seen in the acquired data (Fig. 2), which are the result of the movement of the bees in relation to the movement of the scanner.
Training settings: The machine learning model was trained using a RF classifier with 100 trees, with a maximum tree depth which is expanded until all leaves are pure or the minimum number of samples required to split a node (i.e., 2) is reached. Furthermore, the minimum number of samples per leaf was set to 1. The dataset was split into training and test data by a 80/20 ratio, which meant using eight scenes for training and the other two for testing. Given the imbalanced nature of the dataset, where hornets and bees are underrepresented compared to the miscellaneous class (with ~3,000 hornet points, ~2,000 bee points, compared to ~2,500,000 points classified as miscellaneous), class weights were applied during training. The class weights were computed automatically based on the inverse

class frequencies to assign higher importance to the minority classes (i.e., bees and hornets). This approach ensured that the classifier did not favor the majority class, thereby improving the classification performance for the underrepresented classes.

3.2.3 Clustering Algorithm

In order to identify individual bees as objects, it was necessary to not only identify single points as bees, but also to group those single points into distinct bee objects and to confirm that they were indeed bees. Consequently, the entire point cloud was divided into clusters based on local neighborhood relations with the assistance of a Density-Based Spatial Clustering of Applications with Noise (DBSCAN) algorithm (step 8 in Fig 4) (Deng, 2020). The DBSCAN method employs a proximity-based approach to group points. If a point satisfies the condition that it was within the sphere (r_s) and there were at least *n* points in the sphere (min_{sphere}) and no more than *m* points (max_{sphere}), then all neighboring points were labelled with the same cluster ID. By doing this the entire point cloud was then divided into distinct clusters.

Parameter settings: The resulting values of $r_s = 5$ cm, $min_{sphere} = 1$ pt., $max_{sphere} = 1{,}000$ pts. were determined by counting the points representing a single insect by hand (Fig. 2).

Object-based identification criteria: In the final step, the cluster was definitively identified as a bee or hornet by applying a straightforward logical operator that necessitated the fulfilment of several conditions to classify the cluster as a bee or hornet (step 9 in Fig. 4). From an implementation perspective, the following conditions must be met: In order for a cluster to be identified as a bee, it was first necessary that the number of points classified as bee (bee_{count}) in the cluster in question exceeded the number of points classified as hornet ($hornet_{count}$) within the same cluster ($bee_{count} > hornet_{count}$). And for a cluster to be identified as a hornet the number of points assigned to the hornet category within the cluster had to exceed the number of points assigned to the bee category ($hornet_{count} > bee_{count}$). Furthermore, the following conditions had to be met:

$$\left.\begin{array}{c}\text{bee:}\\ n_{\text{bee}} \leq \text{cluster}_{\text{size}} \leq m_{\text{bee}}\\ \wedge\\ \text{bee}_{\text{count}} \geq (p_{\text{bee}} \cdot \text{cluster}_{\text{size}})\end{array}\right| \begin{array}{c}\text{hornet:}\\ n_{\text{hornet}} \leq \text{cluster}_{\text{size}} \leq m_{\text{hornet}}\\ \wedge\\ \text{hornet}_{\text{count}} \geq (p_{\text{hornet}} \cdot \text{cluster}_{\text{size}})\end{array} \tag{8}$$

where $cluster_{size}$ = number of points in the inquired cluster
bee_{count} = number of points classified as bees in the inquired cluster
n_{bee} = minimum number of points in cluster
m_{bee} = maximum number of points in cluster
p_{bee} = threshold value (percentage) for the number of bees in relation to the cluster size
n_{hornet} = minimum number of points in cluster
m_{hornet} = maximum number of points in cluster
$hornet_{count}$ = number of points classified as hornet in the inquired cluster
p_{hornet} = threshold value (percentage) for the number of bees in relation to the cluster size

If these conditions were satisfied, the cluster was either classified as a single and distinct bee or as a single and distinct hornet. Furthermore, the spatial center of gravity, inclusive of all points within a positively identified cluster, was calculated to generate a new 4D dataset (3D + time) comprising of points that represent individual and distinct bees and hornets. Additionally, the ID of the cluster, the species, the number of classified bees/hornets, the total number of points per cluster, as well as the mean and variance of all features were stored in the new point cloud. Based on the acquired data and testing of different values, it was determined that the optimal parameters for identifying single honey bees were $n_{bee} = 1$, $m_{bee} = 75$, and $p_{bee} = 0.1$ and for identifying hornets $n_{hornet} = 10$, $m_{hornet} = 850$, and $p_{hornet} = 0.25$, as compared to other parts of the scan, such as trees, plants, the hive, and other animals. When using a different measurement setup those parameter can be fine-tuned according to the point-wise representation of the bees/hornets in the scans.

3.3 Error Assessment

In order to assess the error rate of the detection algorithm, it was necessary to ascertain the number of bees and hornets that were correctly identified as such. This was achieved through a visual comparison between the original point cloud and the processed, newly generated point cloud, which consists only of points representing individual, distinct bees and hornets. As the individual bees and hornets were readily discernible to the human eye within the original point cloud, the number of visually identifiable bees/hornets and the number of bees/hornets identified by the algorithm were determined. Additionally, the true positive, false positive, and false negative classifications were recorded. To obtain a reliable estimation of the quality of the detection algorithm, it is necessary to have a sufficient sample size of visual compared epochs in the time series. Accordingly, the requisite sample size was estimated with the finite population correction (Bishop, 2006) to ensure a statistically robust assertion with a confidence level of 95% and an error margin of ±5%. With a total of 225 epochs, the sample size that had to be visually verified is at least 120 epochs. To assess the efficacy of the detection algorithm, four key metrics were employed: accuracy, precision, recall and F1-score (Bishop, 2006).

4. Results

4.1 Random Forest Model Training

The trained RF classifier showed high accuracies. The performance of the model was evaluated through a visual comparison (Fig. 6) and the analysis of confusion matrices over ten random scenes, which were not used for training. For the classification of bees, the mean accuracy, mean precision, and mean recall are 92.23% ± 2.25%, 96.61% ± 1.07%, and 91.04% ± 2.34%, respectively. For the classification of hornets, the mean

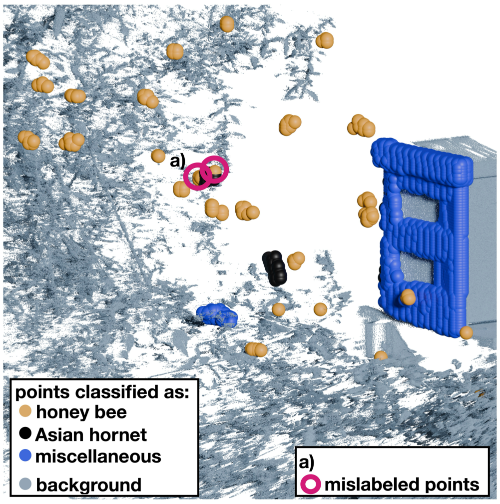

Figure 6. Classification of point cloud from epoch (15:51:56), which was not used for training the random forest classifier.

accuracy, mean precision, and mean recall are 85.61% ± 2.75%, 89.93% ± 2.41%, and 81.02% ± 3.03%, respectively. These high values must be viewed with caution, given the limited size of the test set. Interestingly according to the RF feature importance, the most relevant ones were: eigenentropy (0.34), omnivariance (0.25) and density (0.22).

The misclassification of points, as shown for a single epoch (Fig. 6), which in reality belonged to a hornet but were classified as bee, did not affect the overall correct identification of the hornet. This is because the point cluster was still identified as a hornet, as more than 85% of the points within the cluster were classified as points of the hornet class (Fig. 6 a). By this, the object-based identification criteria for a hornet (Eq. 8) were met. Given the high mean accuracy, precision, and recall, it can be reasonably concluded that the RF classifier is an appropriate method for classifying points in a point cloud as bees and hornets.

4.2 Time Series

By applying the bee detection algorithm to the entire dataset (225 epochs), a time series has been determined in which the number of bees and hornets in front of the hive (1.60 x 1.99 x 1.02m) was calculated every 30 seconds. In total 7,084 bee and 296 hornet observations were counted over the 112.5-minute time span. The resulting data is presented in Fig. 7 a) and b).

To conduct an initial analysis of the time series, the time series was subdivided into bins of 300 s and the total number of bee and hornet observations per bin (i.e., during the 300 s period) was then calculated. This provides an aggregated count of insect observations while maintaining the 2 Hz temporal resolution. However, it must be critically noted that the first and last bin is lower than the actual value due to the calculation method. The results are presented in Fig. 7 c) and d), which clearly demonstrate a discernible trend, particularly in the time series aggregated over 300 s, although it is already perceptible in the original time series.

A second analysis of the time series demonstrates the positions of all bees and hornets aggregated over the entire time series, thereby providing insight into the spatial distribution of bees and hornets over the 112.5-minute span. To enhance the visual representation of the results, the number of neighboring distinct insects for each insect (i.e., bee and hornet) within a radius of 0.2 m was calculated (Fig. 8 and 9).

The mapping of bees and hornets in space and time provides a basis for a more profound understanding of their flight patterns and insights into their spatio-temporal behavior, clearly indicating 3D spatial activity zones. As illustrated in Fig. 8, the bees and hornets exhibit a pronounced concentration in front of the hive and an elongated corridor leading to the hive is clearly visible over the observation period. This phenomenon can be attributed to four primary factors. Firstly, bees frequently congregate in front of their hive to patrol or go on orientation flights (Sun and Gaydecki, 2021). Secondly, this area is, where they tend to decelerate after returning to the hive (Sun and Gaydecki, 2021), a phenomenon that could be observed with our experiments. Additionally, the slowing down of the insects increases the probability of capturing them with TLS. Thirdly, the trajectory of the corridor appears to be largely influenced by the surrounding obstructions, including the trees and buildings adjacent to the hive, the fence at the front, and the branches above (Fig. 1). Fourthly, the area directly in front of the hive is where the hornets were observed to attack bees in the field.

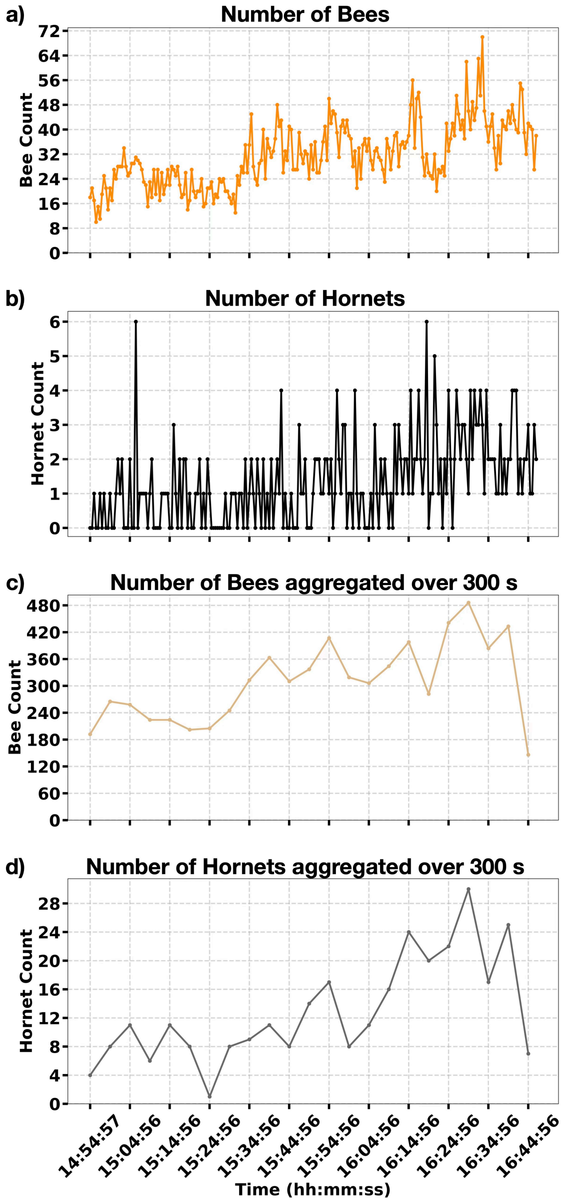

Figure 7. a) Number of bees b) number of hornets c) aggregated count of bees over 300 s and d) aggregated count of hornets over 300 s in examined area over time.

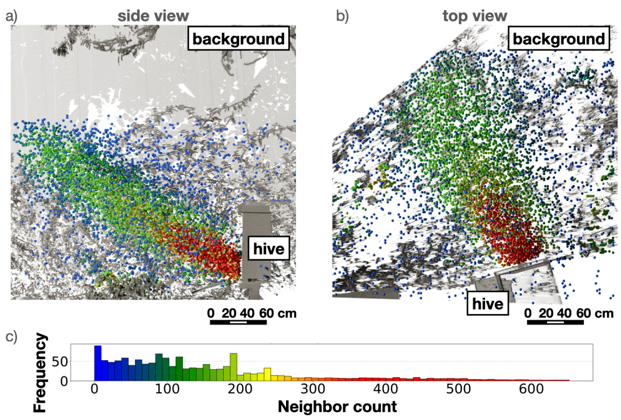

Figure 8. Aggregated positions of bees and hornets over the whole time series (colored by the number of neighboring bees and hornets within a 0.2 m radius to query insect).

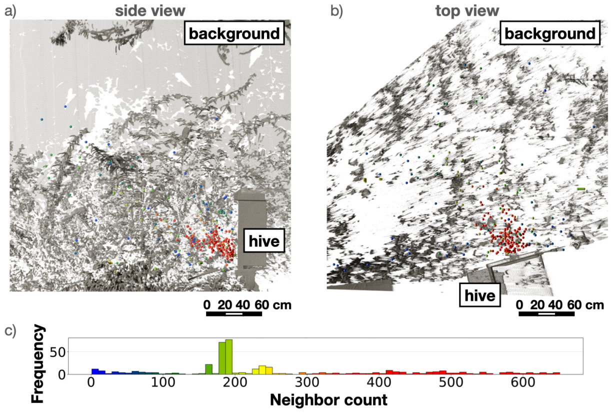

Figure 9. Aggregated positions of hornets over the time series (colored by the number of neighboring bees and hornets within a 0.2 m radius to query hornet).

The phenomenon of hornets attacking in the vicinity of the hive is clearly visible in Fig. 9, which depicts the Asian hornets and demonstrates their tendency to congregate in proximity to the hive entrance. In response to such attacks by the Asian hornet, honey bees typically increase the number of drones in front of the hive to defend themselves (Chauzat and Martin, 2009). This can be seen, when examining the aggregated data for hornets and bees (Fig. 7 c and d), where it becomes evident that an elevated hornet count is associated with a corresponding increase in bee numbers. For instance, between 15:04:57 and 15:24:57, 26 hornet and 790 bee observations were recorded, whereas between 16:04:57 and 16:24:57, 134 hornet and 1447 bee detections were observed.

4.3 Errors

The total number of identifiable bees (i.e., by visually counting the insects in the images captured by the scanner) in the test set is 3448 and the total number of detected bees (i.e., by our proposed algorithm) is 3417. Thereof 3387 were classified as true positives, 30 as false positives, and 61 as false negatives as well as 85 identifiable hornets and 94 detected hornets whereof 79 are true positives, 15 false positives and 8 false negatives. For the identification of bees, the mean accuracy, mean precision, and mean recall are 97.44% ± 0.32%, 99.07% ± 0.23%, and 98.35% ± 0.25%, respectively. For the identification of hornets, the mean accuracy, mean precision, and mean recall are 87.71% ± 2.66%, 67.65% ± 4.97%, and 94.91% ± 1.84%, respectively. Corresponding to an F1-score of 0.987 for the bee identification and 0.79 for the hornet identification. The results demonstrate a high degree of accuracy in the detection algorithm. Notably, for the bees, the precision is higher than the recall, indicating that each bee identified as such has a 97.44% probability of also being a real bee. Conversely, there is an 98.35% probability that the number of bees determined by the algorithm accurately represents the actual number of bees present. Contrary for the hornets the recall is higher than the precision.

5. Discussion

It is important to note that due to the 30-second scanning time, it is highly probable that some bees were captured multiple times, while others may not be captured despite being present within the scanned area. This is because the scanner does not sample the whole area, which is to be scanned, at the exact same time and therefore, the number of bees present is only an estimation. The degree of over- or underestimation is influenced by many factors such as the specific constellation of flight paths and TLS scan pattern. This issue could be addressed by employing multiple scanners with complementary scan patterns or significantly reducing the scan time while maintaining a comparable resolution (i.e., narrowing the scanned area). But this problem is actually overcome by the assumption that for most applications, whether scientific or applied, the relative change is of greater importance or just as reliable as the absolute number of bees. This is particularly relevant in light of the fact that the average rate of over- and underestimation is likely to remain approximately the same.

In the future, the combination of LiDAR and video-based methods has the potential to reveal the complementary strengths of both approaches. We expect that the use of video could be helpful in the close vicinity of the hive and will result in a higher temporal resolution.

The efficacy and accuracy of the distinction between two different species of insects (*A. mellifera* and *V. velutina*) with the proposed algorithm demonstrate the potential for diverse future applications. For example, the study of interspecies behavior of insects, such as the attacking of honey bees by predator insects (e.g., *Vespa velutina*), would be particularly interesting because, as of today, only limited research has been conducted on the topic of flying patterns in moments of defense of the colony by drones. This could reveal a lot about defense and attacking strategies of different insect species. Additionally, the algorithm could provide beekeepers with near real-time information about attacks on their colonies, such as those by *Vespa velutina*, which could assist them in combating disruptive stress caused by predator insects. Furthermore, effects caused by the movement of the bees and hornets (e.g., flying direction or wing movement) which can result in "ghost points" in the point cloud and could disrupt the detection algorithm, are eradicated by the clustering algorithm leading to a low rate of overestimation.

To illustrate, in the context of a management and early warning system for beekeepers, the ability to discern relative change in near real-time is of greater use than the absolute number, which would necessitate a more substantial measurement endeavor to ascertain. This is because the activity and the relative change with a high temporal resolution (i.e., near real-time) can be indicative of honey production, pollination activity, and the survival of the colony (Vercelli et al., 2021).

6. Conclusion

It is possible to use terrestrial LiDAR data to detect and identify individual bees and hornets within the point clouds. The efficacy of the identification algorithm is underscored by its high mean accuracy, mean recall as well as F1-scores (for bees: accuracy = 97.44% ± 0.32%, recall = 98.35% ± 0.25%, and F1 = 0.987, and for hornets: accuracy = 87.71% ± 2.66%, recall = 94.91% ± 1.84% and F1 = 0.79). As demonstrated by the presented time series of 225 epochs in intervals of 30 s and a total of 56,721,201 points, we were able to reduce the data amount while simultaneously extracting the information of 7,084 bee observations and 296 hornet observations from the point cloud time series. Furthermore, this data can be utilized to ascertain the activity zones and temporal dynamics of the bees and hornets, facilitating a deeper understanding of their behavioral patterns. For example, with our novel observation strategy we could observe and quantify a distinct increase of bee presence with the occurrence of hornets in front of the hive.

The insights that are made possible with 4D LiDAR-based bee monitoring can be integrated into improved management and conservation strategies in the future, while also offering a novel tool for the investigation spatial and temporal behavior of insects in addition to the already available video-based approaches. The here presented method of detecting insects (i.e., honey bees and Asian hornets) in LiDAR point clouds is able to measure them in space and time - allowing for a new method in a field of research, concerning the spatio-temporal patterns of insects and pave the way for a range of innovative applications.

7. Acknowledgements

We want to thank Eva-Maria Elfner-Häfele as well as the team of the zoo of Heidelberg for their cooperation in conducting the measurements with their bees. This research was funded by the Deutsche Forschungs-gemeinschaft (DFG, German Research Foundation) – no. 496418931 (VirtuaLearn3D), no. 528521476 (Fostering a community-driven and sustainable HELIOS++ scientific software) and no. 535733258 (Extract4D project). This work is funded by the BMBF AIMon 5.0: Project no. 02WDG1696. The Federal Ministry of Education and Research (BMBF) is funding the AIMon 5.0 project within the funding measure 'Digital GreenTech – Environmental Engineering meets Digitalisation' as part of the 'Research for Sustainability (FONA) Strategy'.

References

Alfio, V. S., Pepe, M., Constantino, D., 2024. The Use of Random Forest for the Classification of Point Cloud in Urban Scene. *International Journal of Engineering Trends and Technology*, 72(3), 1-9.

Azmy, S. N., Sah, S. A., Shafie, N. J., Ariffin, A., Majid, Z., Ismail, M. N., Shamsir, M. S., 2012. Counting in the dark: non-intrusive laser scanning for population counting and identifying roosting bats. *Scientific Reports*, 2(524), 1-4.

Bishop, C. M., 2006. *Pattern Recognition and Machine Learning*. Springer, New York.

Breiman, L., 2001. Random Forests. *Machine Learning*, 45, 5-32.

Brown, M. J. F., Paxton, R. J., 2009. The conservation of bees: a global perspective. *Apidologie*, 40, 410-416.

Chauzat, M. P., Martin, S. J., 2009. A Foreigner in France: Biological Information about the Asian Hornet Vespa Velutina, a recently introduced species. *Biologist*, 56(2), 86-91.

Chen, H., Li, M., Månefjord, H., Travers, P., Salvador, J., Müller, L., Dreyer, D., Alison, J., Høye, T. T., Hu, G., Warrant, E., Brydegaard, M., 2024. Lidar as a potential tool for monitoring migratory insects. *IScience*, 27(5), 1-12.

Deng, D., 2020. DBSCAN Clustering algorithm based on density. *7th International Forum on Electrical Engineering and Automation (IFEEA)*, Hefei, China, 949-953.

Griffiths, D., Boehm, J., 2019. A Review on Deep Learning Technology for 3D Sensed Data Classification. *Remote Sensing*, 11(12), 2-29.

He, X.-J., Tian, L.-Q., Wu, X.-B., Zeng, Z.-J., 2023. RFID monitoring indicates honeybees work harder before a rainy day. *Insect Science*, 23, 157-159.

Hung, K., Kingston, J., Albrecht, M., Holway, D., Kohn, J., 2018. The worldwide importance of honey bees as pollinators in natural habitats. *Proceedings of the Royal Society Biological Sciences*, 285(1870), 2017-2140.

Mohamed, M., Morsy, S., El-Shazly, A., 2023. Improvement of 3D LiDAR point cloud classification of urban road environment based on random forest classifier. *Geocarto International*, 37(27).

Pertischak, H., 2021. *Welche Wildbiene ist das?* Kosmos.

Rodet, G., Henry, M., 2014. Analytic partitioning of honeybee (Apis mellifera L.) flight activity at nest entrance: adaptation and behavioural inertia in a changing environment. *Ecological Research*, 29, 1043-1051.

Ropars, L., Dajoz, I., Fontaine, C., Muratet, A., Geslin, B., 2019. Wild pollinator activity negatively related to honey bee colony densities in urban context. *PLoS One*, 14(9), e0222316.

Rydhmer, K., Prangsma, J., Brydegaard, M., Smith, H. G., Kirkeby, C., Schmidt, I. K., Boelt, B., 2024. Scheimpflug lidar range profiling of bee activity patterns and spatial distributions. *Animal Biotelemetry*, 10(14), 1-13.

Shimasaki, K., Jiang, M., Takaki, T., Ishii, I., Yamamoto, K., 2020. HFR-Video-Based Honeybee Activity Sensing. *Institute of Electrical and Electronics Engineers sensors journal*, 20(10), 5575-5587.

Sun, C., Gaydecki, P., 2021. A Visual Tracking System for Honey Bee (Hymenoptera: Apidae) 3D Flight Trajectory Reconstruction and Analysis. *Journal of Insect Science*, 21(2), 1-12.

Tabernig, R., Albert, W., Weiser, H., Höfle, B., 2024. VAPC - Voxel Analysis for Point Clouds. https://github.com/3dgeo-heidelberg/vapc

Tennakoon, S., 2024. Unravelling the impact of climate change on honey bees: an ensemble modelling approach to predict shifts in habitat suitability in queensland, australia. *Ecology and Evolution*, 14(4).

Vercelli, M., Novelli, S., Ferrazzi, P., Lentini, G., Ferracini, C., 2021. A qualitative analysis of beekeepers' perceptions and farm management adaptations to the impact of climate change on honey bees. *Insects*, 12(3), 228.

Weiser, H., Höfle, B. 2024. Virtual laser scanning of dynamic scenes (VLS-4D): Current approaches and future perspectives in remote sensing. *EarthArXiv*.